

See discussions, stats, and author profiles for this publication at: <https://www.researchgate.net/publication/273784349>

A Generic Magnetic Microsphere Platform with “Clickable” Ligands for Purification and Immobilization of Targeted Proteins

ARTICLE in ACS APPLIED MATERIALS & INTERFACES · MARCH 2015

Impact Factor: 6.72 · DOI: 10.1021/acsaami.5b00313 · Source: PubMed

CITATION

1

READS

46

7 AUTHORS, INCLUDING:



[Yu Ding](#)

Fudan University

23 PUBLICATIONS 172 CITATIONS

[SEE PROFILE](#)



[Wuli Yang](#)

Fudan University

154 PUBLICATIONS 4,714 CITATIONS

[SEE PROFILE](#)

A Generic Magnetic Microsphere Platform with “Clickable” Ligands for Purification and Immobilization of Targeted Proteins

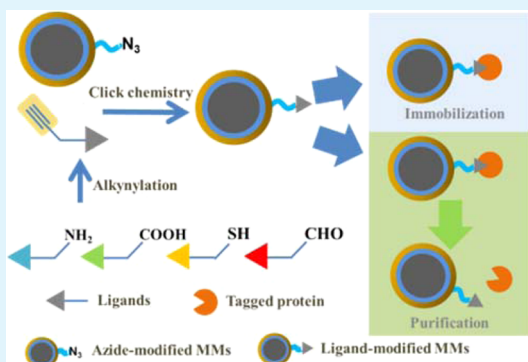
Jin Zheng,[†] Yipeng Li,[‡] Yangfei Sun,[‡] Yongkun Yang,[§] Yu Ding,[‡] Yao Lin,[§] and Wuli Yang*,[†]

[†]State Key Laboratory of Molecular Engineering of Polymers and Department of Macromolecular Science and [‡]School of Life Sciences, Fudan University, No. 220 Handan Road, Shanghai 200433, China

[§]Polymer Program, Institute of Materials Science and Department of Chemistry, University of Connecticut, Storrs, Connecticut 06269, United States

Supporting Information

ABSTRACT: While much effort has been made to prepare magnetic microspheres (MMs) with surface moieties that bind to affinity tags or fusion partners of interest in the recombinant proteins, it remains a challenge to develop a generic platform that is capable of incorporating a variety of capture ligands by a simple chemistry. Herein, we developed core–shell structured magnetic microspheres with a high magnetic susceptibility and a low nonspecific protein adsorption. Surface functionalization of these MMs with azide groups facilitates covalent attachment of alkynylated ligands on their surfaces by “click” chemistry and creates a versatile platform for selective purification and immobilization of recombinant proteins carrying corresponding affinity tags. The general applicability of the approach was demonstrated in incorporating four widely used affinity ligands with different reactive groups ($-\text{CHO}$, $-\text{SH}$, $-\text{COOH}$, and $-\text{NH}_2$) onto the MMs platform for purification and immobilization of targeted proteins. The azide-functionalized MMs would be applicable for a variety of ligands and substrates that are amenable to alkynylation modification.



KEYWORDS: magnetic microspheres, click chemistry, fusion protein, separation, immobilization

1. INTRODUCTION

Proteins have an array of functions in living organisms, such as chemical catalysis, DNA replications, stimuli responses, and molecular transport.¹ Analyzing protein composition, structures, and activities in the intracellular environment requires the development of new high-throughput separation and identification methods. However, proteins of interest are often mixed with numerous other biological components in the cells that complicate the identification and analysis of target proteins.² Development of new tools in fast protein purification and immobilization are relevant for both basic research and industrial applications.

Recombinant proteins, carried by a recombinant DNA, usually include two parts, affinity tag and target protein.³ Affinity tags and other types of genetically engineered fusion partners such as His-tag,⁴ GST-tag,⁵ SNAP tag,⁶ Halo tag,⁷ and Clip tag,⁸ are routinely employed in the production of recombinant proteins, to facilitate easy detection and purification of proteins, or to improve the solubility and stability of proteins.⁹ Magnetic microspheres (MMs) have received increasing attention in many fields owing to the excellent magnetic response and easy operation.¹⁰ They allow intricate manipulation to be carried in biological systems, which can be easily implemented by an external magnetic field and is especially applicable for proteomics research.¹¹ Recently, many

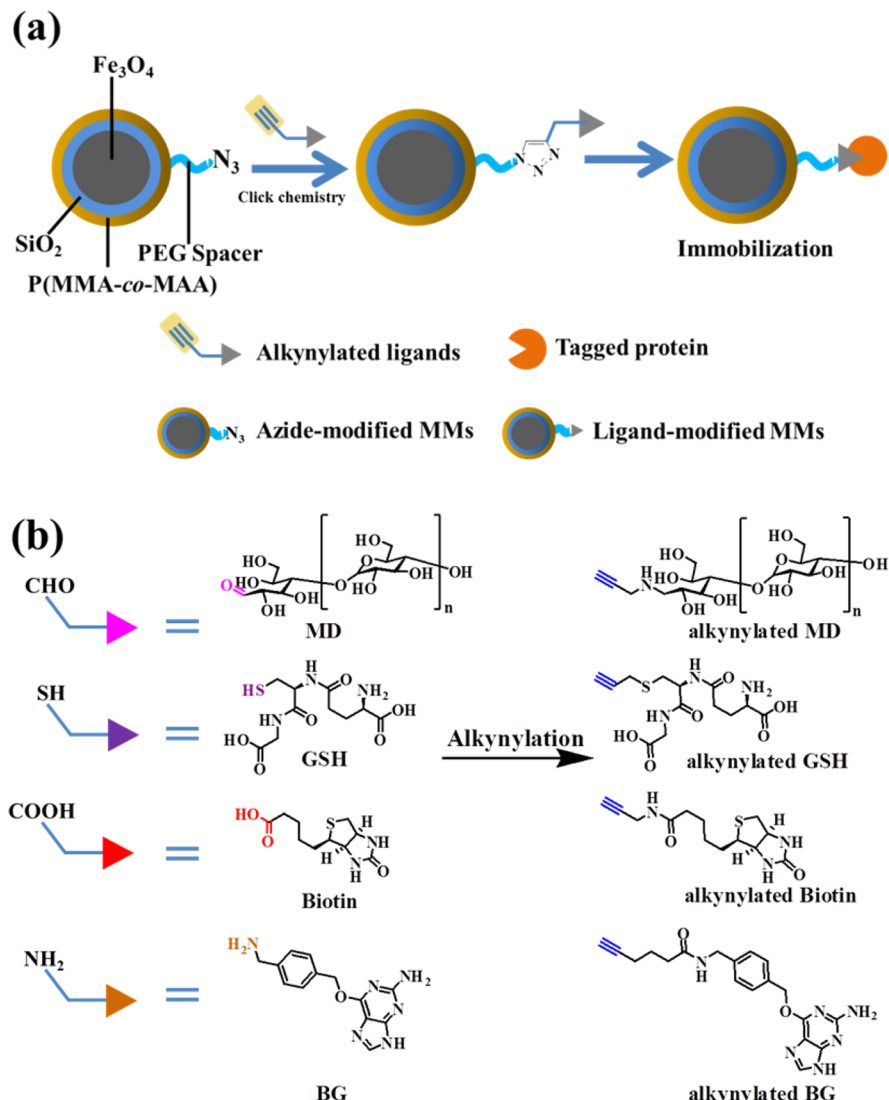
attempts have been made to develop MMs with surface moieties that selectively bind to the affinity tags or fusion partners in recombinant proteins, as this provides a simple route for enrichment and manipulation of the proteins under a magnetic field, either *in vitro* or *in vivo*.^{12–15} For example, Bruening and co-workers synthesized a class of poly(2-hydroxyethyl methacrylate)-grafted MMs that can be subsequently functionalized with nitrilotriacetate-Ni²⁺ for capturing His-tagged proteins from cell extracts.¹⁶ Xu developed glutathione-decorated MMs for directly sorting GST-tagged proteins inside live cells.¹⁷ Zhang utilized Avicel-containing MMs to co-immobilize different types of recombinant phosphorylases that contain a cellulose binding domain (CBD) and utilize the synergistic reactions of the enzyme complexes to convert cellulose to starch.¹⁸ While it is envisioned that more MMs will be developed to target individual affinity tags or fusion partners of interest in the recombinant proteins, a generic platform that is capable of incorporating a variety of capture ligands by a simple chemistry is highly desired.

Herein, we report a generic MMs-based platform for enrichment and immobilization of different types of tagged

Received: January 13, 2015

Accepted: March 18, 2015

Scheme 1. (a) Functionalization of MMs with “Clickable” Ligands to Capture Corresponding Tagged Proteins, and (b) the Alkylation of Different Ligands



proteins (Scheme 1). Core–shell–shell MMs with high magnetic susceptibility and low nonspecific binding of proteins were synthesized and surface-functionalized with azide groups. “Click” chemistry was utilized to conjugate specific affinity ligands onto the surface of MMs for immobilization of tagged proteins.^{19,20} Four widely used affinity ligands, including maltodextrin (MD) that binds to maltose-binding protein,²¹ glutathione (GSH) that binds to GST-tagged protein,²² biotin that binds to streptavidin (SA),²³ and *O*⁶-(4-aminomethylbenzyl) guanine (BG) that binds to SNAP-tagged protein,²⁴ were successfully employed to the MMs platform for immobilization of the corresponding proteins from cell lysates. As shown in Scheme 1, the precursors of the four affinity ligands present widely different reactive groups ($-\text{CHO}$, $-\text{SH}$, $-\text{COOH}$, and $-\text{NH}_2$). The fact that all these ligand precursors can undergo the alkylation reaction and then “click” to the surface of MMs demonstrates the general applicability of the approach. The MMs, which can be functionalized to target a variety of different recombinant proteins, may find applications in protein purification, cell biology, biotechnology, and the high-throughput sensing or screening devices.

2. EXPERIMENTAL SECTION

2.1. Chemicals and Reagents. Aqueous ammonia solution (25%), ferric chloride (FeCl_3), methyl methacrylate (MMA), methylacrylic acid (MAA), tetraethyl orthosilicate (TEOS), 3-(trimethoxysilyl) propyl methacrylate (MPS), sodium acetate (NaOAc), sodium dodecyl sulfate (SDS), ethylene glycol, trisodium citrate dehydrate ($\text{C}_8\text{H}_5\text{Na}_3\text{O}_7 \cdot 2\text{H}_2\text{O}$), sodium azide (NaN_3), sodium borohydride (NaBH_4), maltose, potassium persulfate (KPS), *p*-toluenesulfonyl chloride (TsCl), triethylamine, *N*-(3-(dimethylamino)propyl)-*N'*-ethylcarbodiimide hydrochloride (EDC-HCl), poly(ethylene glycol) ($M_w = 600$, PEG₆₀₀), triphenylphosphine (Ph_3P), anhydrous ethanol, dichloromethane (DCM), and ethyl acetate (EtOAc) were purchased from Sinopharm Chemical Reagent Co. Ltd. DL-dithiothreitol (DTT), ethylene glycol dimethacrylate (EGDMA), tris(hydroxymethyl)aminomethane hydrochloride (Tris-HCl), glutathione (GSH), and other biological reagents were obtained from Sigma-Aldrich. Maltodextrin (MD, DE = 8–10) were obtained from Shandong Xiwang pharmaceutical Co, Ltd. The other chemicals were of analytical grade.

2.2. Preparation of Fe_3O_4 Particles and $\text{Fe}_3\text{O}_4@\text{SiO}_2$ Microspheres. The Fe_3O_4 particles were prepared by solvothermal reaction,²⁵ and the detailed experimental processes were provided in our previous work.²⁶

2.3. Preparation of $\text{Fe}_3\text{O}_4@\text{SiO}_2$ Microspheres. The $\text{Fe}_3\text{O}_4@\text{SiO}_2$ microspheres were prepared by the sol-gel approach, and the detailed experimental processes were also provided in our previous work.²⁶

2.4. Preparation of $\text{Fe}_3\text{O}_4@\text{SiO}_2$ -MPS Microspheres. The surfaces of $\text{Fe}_3\text{O}_4@\text{SiO}_2$ microspheres were modified with MPS. Briefly, 100 mL of deionized water, 400 mL of ethanol, 10 mL of aqueous ammonia, and 2.5 mL of MPS were mixed with 250 mg of $\text{Fe}_3\text{O}_4@\text{SiO}_2$ microspheres. Then, the mixture was stirred vigorously for 24 h at 40 °C. The $\text{Fe}_3\text{O}_4@\text{SiO}_2$ -MPS microspheres were washed with ethanol by magnetic separation and dispersed in 40 mL of ethanol.

2.5. Preparation of $\text{Fe}_3\text{O}_4@\text{SiO}_2@P(\text{MMA}-co-\text{MAA})$ Microspheres. The $\text{Fe}_3\text{O}_4@\text{SiO}_2@P(\text{MMA}-co-\text{MAA})$ magnetic microspheres were prepared by a seed emulsion polymerization.²⁷ Briefly, 30 mL of deionized water and 6.0 mg of SDS were mixed with 5 mL of dispersion of $\text{Fe}_3\text{O}_4@\text{SiO}_2$ -MPS (5 mg mL⁻¹). After stirring for 30 min, 95 mg of MMA, 5 mg of MAA, 20 μL of EGDMA, and 4 mg of KPS were added to the mixture. Then the polymerization was performed at 75 °C for another 5 h. The obtained $\text{Fe}_3\text{O}_4@\text{SiO}_2@P(\text{MMA}-co-\text{MAA})$ microspheres were washed repeatedly with ethanol through magnetic separation.

2.6. Preparation of PEG Spacer $\text{NH}_2-\text{PEG}_{600}-\text{N}_3$. PEG₆₀₀ (30.0 g, 50 mmol) and TsCl (11.95 g, 104 mmol) were dissolved in 100 mL of THF, and the solution was cooled to 0 °C under N₂. Triethylamine (16.2 mL, 120 mmol) was added dropwise to the reaction, and the mixture was then warmed to room temperature and stirred for 12 h. After that, 125 mL of 5% NaHCO₃ was added, followed by NaN₃ (8.33 g, 128 mmol). To distill the THF, the content was refluxed for 7 h. After it cooled, the mixture was extracted with EtOAc, and the combined organic layers were dried over Na₂SO₄. The crude product was purified by silica column chromatography to give N₃-PEG₆₀₀-N₃ (22.75 g, 70% yield).

N₃-PEG₆₀₀-N₃ (12.0 g, 20 mmol) was dissolved in the mixture of 150 mL of EtOAc and 60 mL of 1 M HCl. Ph₃P (5.2 g, 20 mmol) was added. The mixture was stirred for another 12 h. The pH value was adjusted to 14 by 1 M NaOH, and then the mixture was extracted with DCM. The combined organic layers were dried by Na₂SO₄. The crude product was purified by silica gel column chromatography to give NH₂-PEG₆₀₀-N₃ (9.0 g, 75% yield).²⁸

2.7. Preparation of $\text{Fe}_3\text{O}_4@\text{SiO}_2@P(\text{MMA}-co-\text{MAA})$ -PEG-N₃ (N₃-MMs). Fe₃O₄@SiO₂@P(MMA-co-MAA) (50 mg) was dispersed into the mixture of 10 mL of DMF and 10 mL of pH 7.4 phosphate buffer solution (PBS), then EDC-HCl (10 mg) and NHS (10 mg) were added. The reaction was stirred for 30 min under N₂. Then NH₂-PEG₆₀₀-N₃ (20 mg) was added, and the mixture was stirred for another 24 h at room temperature. The final products (azide-modified MMs) were collected by magnetic separation and redispersed in 10 mL of ethanol.

2.8. Preparation of Alkynylated Maltodextrin. Maltodextrin (MD, 1.0 g) and 3-amino-1-propyne (0.5 g) were added into 50 mL of ethanol. The mixture was continuously stirred at 70 °C for 6 h. Then, the mixture was stirred at room temperature, and NaBH₄ (0.3 g) was added and reacted for another 12 h. The solvent was removed in vacuum, and the crude products were collected for the next step use without further purification.

2.9. Preparation of Alkynylated Glutathione. Glutathione (GSH, 307 mg) was added into 10 mL of 0.4 M Ba(OH)₂ solution under N₂, then propargyl bromide (110 mg) was added and reacted for 24 h. After removing the solvent in vacuum, the crude products were collected for the next step use without further purification. ¹H NMR (D₂O, 400 MHz): δ = 2.07 (dd, 2H), 2.45 (m, 2H), 2.60 (dd, 1H), 2.92 (dd, 1H), 3.18 (dd, 1H), 3.29 (m, 2H), 3.70 (m, 3H), 4.65 (dd, 1H).

2.10. Preparation of Alkynylated Biotin. Biotin (244 mg, 1 mmol) was dissolved in 10 mL of DMF. Then EDC-HCl (191 mg, 1 mmol), TEA (100 μL), and NHS (99 mg, 1 mmol) were added and reacted for 2 h. Then 3-amino-1-propyne (50 μL) were added and stirred for another 12 h. The solvent was evaporated in vacuum, and the crude product was purified by silica column chromatography to

give alkynylated biotin as a white solid (225 mg, 0.80 mmol, 80% yield). ¹H NMR (DMSO-d₆, 400 MHz): δ = 1.25–1.60 (m, 6H), 2.05 (t, 2H), 2.55 (d, 1H), 2.80 (m, 1H), 3.08 (m, 1H), 3.82 (d, 2H), 4.10 (m, 1H), 4.28 (t, 1H), 6.36 (s, 1H), 6.43 (s, 1H), 8.21 (s, 1H).

2.11. Preparation of Alkynylated O⁶-(4-Aminomethylbenzyl)guanine. 5-Hexynoic acid (70 mg, 1 mmol) was dissolved in 10 mL of dry DMF under N₂. Then EDC-HCl (191 mg, 1 mmol), TEA (100 μL), and NHS (99 mg, 1 mmol) were added and reacted for 2 h. Then BG (270 mg, 1 mmol; see preparation details in Supporting Information) was added and stirred for another 12 h. The solvent was removed in vacuum, and the crude product was purified by silica column chromatography to give alkynylated BG as a pale solid (237 mg, 0.65 mmol, 65% yield). ¹H NMR (DMSO-d₆, 400 MHz): δ = 1.67 (m, 2H), 2.22 (m, 4H), 2.79 (s, 1H), 4.21 (s, 2H), 5.43 (s, 2H), 6.26 (s, 2H), 7.24 (m, 4H), 7.45 (d, 1H), 7.76 (s, 1H), 8.33 (s, 1H), 12.40 (s, 1H).

2.12. Preparation of Ligand-Modified MMs. Azide-modified MMs (25 mg) and 10 mg of alkynylated MD were mixed in 10 mL of DMF and 10 mL of pH 7.4 PBS under N₂. Then CuSO₄·5H₂O (5 mg) and sodium ascorbate (10 mg) were added and reacted for 24 h at room temperature. The resulting MD-modified magnetic microspheres (MD-MMs) were washed repeatedly and collected by magnetic separation.

The preparation process for GST-modified magnetic microspheres (GSH-MMs), biotin-modified magnetic microspheres (biotin-MMs), and BG-modified magnetic microspheres (BG-MMs) were same with that of MD-MMs, except the initial recipe was 10 mg of alkynylated GST, 5 mg of alkynylated biotin, and 5 mg of alkynylated BG instead of alkynylated MD, respectively.

2.13. Cloning of MBP-mCherry, GST-mCherry, and SNAP-pre-Cel48F. The plasmid-encoding monomer red fluorescent mCherry was kindly provided by Prof. Roger Tsien's lab in UCSD. Then the MBP-mCherry and GST-mCherry plasmids were constructed by inserting the mCherry CDS to the revised pMal-C2x and pGEX-4T vectors, which contained the MBP and GST tags, respectively. The SNAP-pre-Cel48F plasmid was constructed from SNAP-Cel48F, synthesized by GenScript Corporation. The PreScission protease cleavage site was introduced by PCR between the N terminal processive endocellulase Cel48F protein and C terminal SNAP-tag.²⁹ All the plasmids were verified by sequencing (see CDS in Supporting Information for the amino acid sequence of the protein) and then transformed into BL21 (DE3) pLysS for expression.

2.14. Expression of MBP-mCherry, GST-mCherry, and SNAP-pre-Cel48F. The protein-encoding plasmids were transformed into *E. coli* strain BL21 (DE3) pLysS. After the colony had grown in LB medium with ampicillin by shaking at 37 °C, the bacterial suspension was transferred into a 2 L flask containing 250 mL of autoinduction medium. When the cells had grown to an optical density at 600 nm, temperature was lowered to 19 °C. After 20 h, the cells were collected by centrifugation at 6000 g and stored at -80 °C.

2.15. Purification of MBP-mCherry and GST-mCherry. The collected cells from 1 L of culture were resuspended in 200 mL of buffer A (50 mM Tris-HCl, pH 8.5, 150 mM NaCl, 10% glycerol, and 20 mM imidazole) and lysed by sonication to give the cell lysate.

For MBP-mCherry, 100 μL of MD-MMs (2 mg mL⁻¹) was sedimented in a microcentrifuge tube and washed with 500 μL of MBP binding buffer (200 mM NaCl, 20 mM Tris-HCl, 1 mM DTT, 1 mM EDTA, and pH 7.4) three times. Then 500 μL of cell culture supernatant was mixed with MD-MMs and incubated at 4 °C for 1 h. The supernatant was removed, and the protein-bonded composite microspheres were washed with MBP binding buffer three times. The protein was eluted from MD-MMs with 50 μL of elution buffer (MBP binding buffer containing 10 mM maltose) at 4 °C.

The purification for GST-mCherry was same with that of MBP-mCherry, except the GST binding buffer was 150 mM NaCl, 125 mM Tris-HCl at pH 8.0 and GST elution buffer was 250 mM NaCl, 10 mM Tris-HCl, 50 mM GSH at pH 8.5.

The protein solution was analyzed by sodium dodecyl sulfate polyacrylamide gel electrophoresis (SDS-PAGE). The protein concentration was measured in triplicate by the Bradford method.³⁰

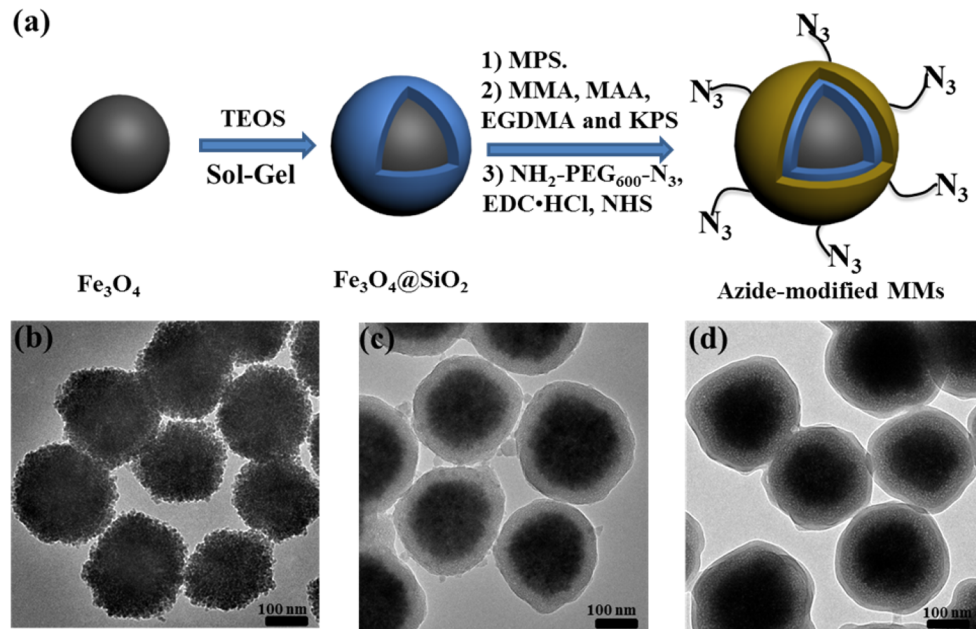


Figure 1. (a) Procedure of preparation of core–shell–shell structured MMs. Representative TEM images of (b) Fe_3O_4 , (c) $\text{Fe}_3\text{O}_4@\text{SiO}_2$, and (d) $\text{Fe}_3\text{O}_4@\text{SiO}_2@\text{P}(\text{MMA}-\text{co-}\text{MAA})$ particles. The scale bars are 100 nm.

GST activity of GST-mCherry was measured by the Glutathione S-Transferase Assay Kit.³¹

2.16. Immobilization of Streptavidin and SNAP-pre-Cel48F. SNAP-pre-Cel48F supernatant was loaded on a 5 mL Ni-NTA superflow column equilibrated by buffer A, then washed by buffer B (50 mM Tris-HCl, pH 8.5, 1 M NaCl, 10% glycerol and 50 mM imidazole), and eluted by elution buffer C (50 mM Tris-HCl, pH 8.5, 300 mM imidazole and 10% glycerol) to give purified SNAP-pre-Cel48F.

Streptavidin and SNAP-pre-Cel48F were mixed and shaken with the Biotin-MMs and BG-MMs, respectively, at 4 °C for 1 h. The supernatant was removed, and the protein-bonded composite microspheres were washed with buffer D (200 mM NaCl, 20 mM Tris-HCl, and pH 7.4) three times.

2.17. Enzyme Activity of Immobilized SNAP-pre-Cel48F. The enzyme activity of SNAP-pre-Cel48F on Avicel was determined by evaluation of the total amount of soluble reducing sugars released at specific time intervals.¹⁵ SNAP-pre-Cel48F was incubated with Avicel (20 mg mL⁻¹) for 0, 1, 6, and 24 h either in the free state or immobilized on the MMs and examined for soluble reducing sugars using ferricyanide assay.³² The final SNAP-pre-Cel48F concentration was 0.03 μM . All measurements were performed in triplicate.

2.18. Characterization. The hydrodynamic diameter and zeta potential of the samples were measured on a dynamic light scattering (DLS) particle size analyzer (Malvern Nano-ZS90). The transmission electron microscopy (TEM) images were performed on a Tecnai G2 20 TWIN transmission electron microscope. Fourier transform infrared (FTIR) spectroscopy spectra were obtained on a Nicolet Nexus-440 FTIR spectrometer. Thermogravimetric analysis (TGA) was performed by a Pyris 1 TGA instrument under air environment with a heating rate of 20 °C min⁻¹. Magnetic property was measured by a vibrating sample magnetometer (VSM) on a model 6000 physical property measurement system (Quantum, U.S.) at 300 K.

3. RESULTS AND DISCUSSION

3.1. Preparation of N_3 -MMs. The synthesis of core–shell–shell MMs involves four steps (Figure 1a). First, a modified solvothermal reaction was used to prepare highly crystalline Fe_3O_4 particles as the core of the MMs.³³ As Fe_3O_4 has relatively weak interactions with organic polymers, an additional layer of SiO_2 was coated onto Fe_3O_4 particles

($\text{Fe}_3\text{O}_4@\text{SiO}_2$) by a sol–gel process for subsequent deposition of polymers. The silica surface was then grafted with MPS to incorporate active C=C bonds, through which a polymer layer was formed by an emulsion polymerization of MMA and MAA ($\text{Fe}_3\text{O}_4@\text{SiO}_2@\text{P}(\text{MMA}-\text{co-}\text{MAA})$). The carboxylic acid groups (–COOH) incorporated on the polymer layer were then activated by EDC·HCl to couple with an amine-functionalized poly(ethylene glycol) molecule that has an azide group at the other end ($\text{NH}_2-\text{PEG}_{600}-\text{N}_3$).³⁴ This final step attached reactive azide groups on the surface of $\text{Fe}_3\text{O}_4@\text{SiO}_2@\text{P}(\text{MMA}-\text{co-}\text{MAA})$ (N_3 -MMs), which can subsequently be used to conjugate a variety of capture ligands carrying alkyne groups by simple click chemistry.³⁵ Figure 1b–d shows the TEM images of Fe_3O_4 ($d = 216 \pm 20$ nm), $\text{Fe}_3\text{O}_4@\text{SiO}_2$ ($d = 251 \pm 23$ nm), and $\text{Fe}_3\text{O}_4@\text{SiO}_2@\text{P}(\text{MMA}-\text{co-}\text{MAA})$ ($d = 263 \pm 25$ nm) obtained at each step. The composition of the polymer layer was optimized to obtain a surface with a low degree of nonspecific protein adsorption.²⁷ The hydrodynamic diameter of Fe_3O_4 was 270 nm, and the zeta potential was –21 mV due to the existence of citrate groups on the surface of Fe_3O_4 (Table 1). With the addition of a SiO_2 shell, the hydrodynamic diameter of $\text{Fe}_3\text{O}_4@\text{SiO}_2$ increased to 328 nm,

Table 1. Particle Size and Zeta Potential of Fe_3O_4 , $\text{Fe}_3\text{O}_4@\text{SiO}_2$, $\text{Fe}_3\text{O}_4@\text{SiO}_2$ -MPS, $\text{Fe}_3\text{O}_4@\text{SiO}_2@\text{P}(\text{MMA}-\text{co-}\text{MAA})$, and N_3 -MMs^a

sample	zeta potential (mV)	hydrodynamic diameter (nm) ^b	PDI ^c
Fe_3O_4	–21	270	0.18
$\text{Fe}_3\text{O}_4@\text{SiO}_2$	–41	328	0.15
$\text{Fe}_3\text{O}_4@\text{SiO}_2$ -MPS	–24	365	0.13
$\text{Fe}_3\text{O}_4@\text{SiO}_2@\text{P}(\text{MMA}-\text{co-}\text{MAA})$	–44	476	0.16
N_3 -MMs	–30	504	0.16

^aAll the data were measured in 0.15 M PBS at pH = 7.4. ^bThe hydrodynamic diameter was measured at 25 °C by DLS. ^cPDI, polydispersity index, PDI = $\langle \mu_2 \rangle / \Gamma^2$.³⁷

and the zeta potential was -41 mV for the existence of silanol groups. After the MMs modified with MPS, the zeta potential of $\text{Fe}_3\text{O}_4@\text{SiO}_2$ -MPS increased to -24 mV. When coating with P(MMA-*co*-MAA), the zeta potential of $\text{Fe}_3\text{O}_4@\text{SiO}_2@P(\text{MMA}-\text{co}-\text{MAA})$ decreased to -44 mV, and the hydrodynamic diameter increased to 476 nm. After coupling with $\text{NH}_2-\text{PEG}_{600}-\text{N}_3$, the hydrodynamic diameter of N_3 -MMs increased to 504 nm, and PDI was 0.16 . The microspheres showed good stability and narrow size dispersion. The hydrodynamic sizes of the microspheres were larger than that shown in TEM image, which was mainly due to the presence of hydrate layer in aqueous environment.³⁶

The surface functionalization of MMs was confirmed by FTIR (Figure 2) and TGA (Figure 3). After coating with SiO_2 ,

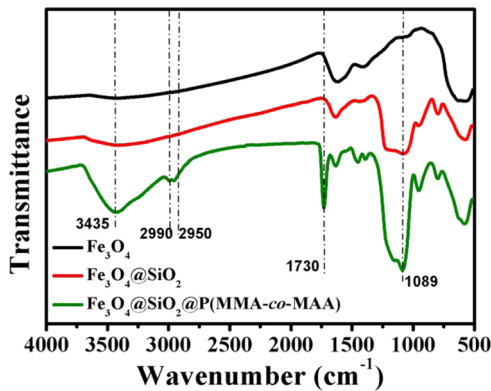


Figure 2. FTIR spectra of Fe_3O_4 , $\text{Fe}_3\text{O}_4@\text{SiO}_2$, $\text{Fe}_3\text{O}_4@\text{SiO}_2@P(\text{MMA}-\text{co}-\text{MAA})$.

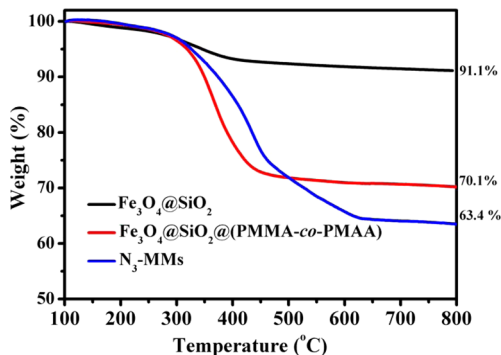


Figure 3. TGA curves of $\text{Fe}_3\text{O}_4@\text{SiO}_2$, $\text{Fe}_3\text{O}_4@\text{SiO}_2@P(\text{MMA}-\text{co}-\text{MAA})$, N_3 -MMs.

the absorption peak for the $\text{Fe}_3\text{O}_4@\text{SiO}_2$ microspheres at 1089 cm^{-1} was attributed to the vibration of Si—O—Si. After coating with P(MMA-*co*-MAA), $\text{Fe}_3\text{O}_4@\text{SiO}_2@P(\text{MMA}-\text{co}-\text{MAA})$ had a peak at 1730 cm^{-1} , which was assigned to C=O bonds. The TGA curves demonstrated that the weight loss of $\text{Fe}_3\text{O}_4@\text{SiO}_2$ was 8.9% , while the weight loss of $\text{Fe}_3\text{O}_4@\text{SiO}_2@P(\text{MMA}-\text{co}-\text{MAA})$ was 29.9% at 800 $^\circ\text{C}$, which indicated that the weight ratio of the polymer shell was 21% . The weight loss of N_3 -MMs was 36.6% , which indicated that weight ratio of the PEG spacer was 6.7% .

The azide groups on the N_3 -MMs were further confirmed by elementary analysis using X-ray photoelectron spectroscopy (XPS; see Table 2). The contents of element Si, and O were 2.5% and 24.6% , respectively, for $\text{Fe}_3\text{O}_4@\text{SiO}_2@P(\text{MMA}-\text{co}-\text{MAA})$.

After coupling of $\text{NH}_2-\text{PEG}_{600}-\text{N}_3$, the content of N emerged to 1.85% .

Table 2. Surface Element Percentage of $\text{Fe}_3\text{O}_4@\text{SiO}_2$, $\text{Fe}_3\text{O}_4@\text{SiO}_2@P(\text{MMA}-\text{co}-\text{MAA})$, N_3 -MMs by XPS

sample	ratio of Si	ratio of O	ratio of N
$\text{Fe}_3\text{O}_4@\text{SiO}_2$	19.0	47.0	
$\text{Fe}_3\text{O}_4@\text{SiO}_2@P(\text{MMA}-\text{co}-\text{MAA})$	2.5	24.6	
N_3 -MMs	4.4	26.4	1.85

The magnetic properties of MMs were characterized by VSM (Figure 4). The saturation magnetization (M_s) value of Fe_3O_4

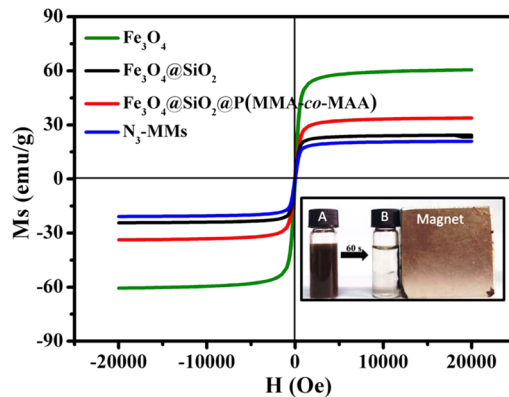


Figure 4. Magnetic hysteresis curves of Fe_3O_4 , $\text{Fe}_3\text{O}_4@\text{SiO}_2$, $\text{Fe}_3\text{O}_4@\text{SiO}_2@P(\text{MMA}-\text{co}-\text{MAA})$, N_3 -MMs. The inset photograph showed two bottles of the sample N_3 -MMs: (A) well-dispersed in water, and (B) attracted microspheres to the side wall by magnetic separation. After slightly shaking, the particles could be redispersed.

was found to be 60 emu g^{-1} . After SiO_2 was coated, the M_s value of $\text{Fe}_3\text{O}_4@\text{SiO}_2$ decreased to 34 emu g^{-1} . After coating with a polymer shell, the M_s value of $\text{Fe}_3\text{O}_4@\text{SiO}_2@P(\text{MMA}-\text{co}-\text{MAA})$ decreased to 23 emu g^{-1} . After reacted with $\text{NH}_2-\text{PEG}_{600}-\text{N}_3$, the M_s value of N_3 -MMs decreased slightly to 20 emu g^{-1} . Although the M_s value of N_3 -MMs decreased significantly compared with the original Fe_3O_4 particles, the magnetic property was large enough to make the microspheres to be separated rapidly, as shown in Figure 4 (the inset). The VSM results also indicated that the magnetic microspheres were superparamagnetic at 300 K.³⁸

3.2. Protein Purification and Immobilization. Click chemistry provides a reliable and efficient tool to the exploitation of functionalized nanomaterials.³⁵ The specific and strong binding interaction is effective in a wide range of pH and temperature. It employs suitable reaction conditions such as aqueous environment, endowing considerable versatility of conjugation for many biomolecules without reducing their activities.³⁹ Furthermore, variety of alkynylated reagents could be easily used for the modification of ligands. To demonstrate the adaptability of using the azide functionalized MMs as a platform to install different capture ligands, we investigated four widely used, commercially available ligands (MD, GSH, biotin, and BG). First, we performed alkynylation reactions from different reactive moieties in the four ligands ($-\text{CHO}$ in MD, $-\text{SH}$ in GSH, $-\text{COOH}$ in biotin, and $-\text{NH}_2$ in BG). The aldehyde group in MD reacted with 3-amino-1-propyne to form the Schiff base and then was reduced by NaBH_4 to obtain alkynylated MD.⁴⁰ Alkynylation of GSH was achieved by

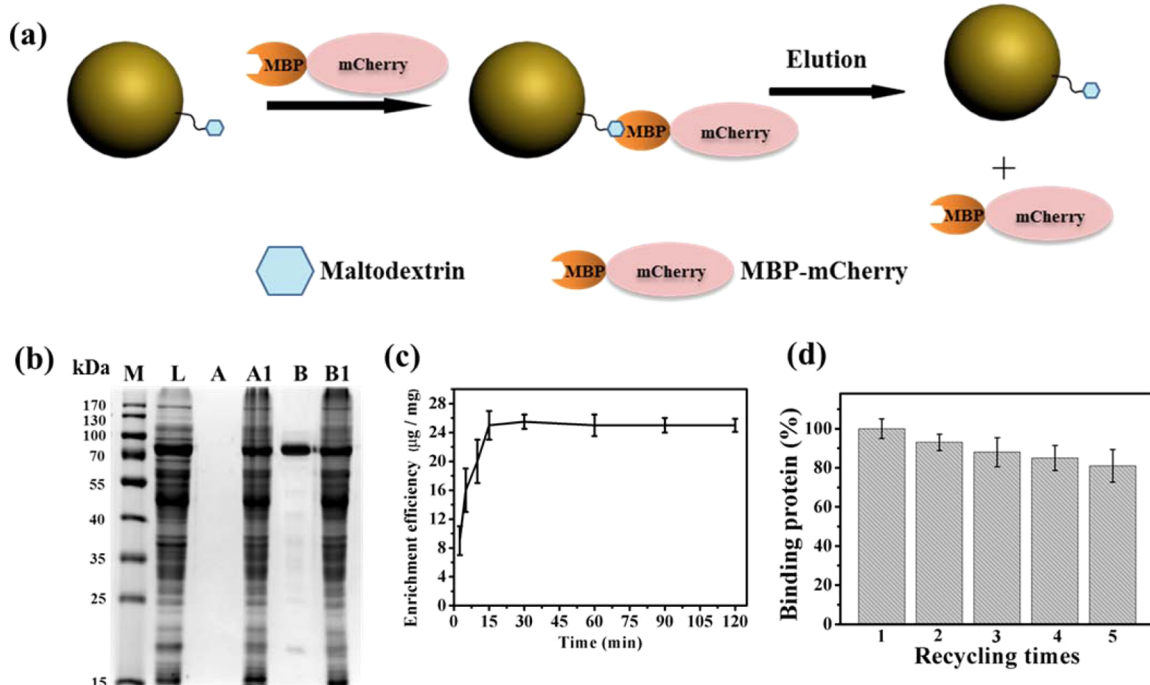


Figure 5. (a) Procedure of purification of MBP-mCherry by MD-MMs, and N₃-MMs were used as control; (b) SDS-PAGE analysis of MD-MMs: lane M, marker; L, crude *E. coli* lysate; A, elution buffer for control; A1, the supernatant solution after the immobilization of crude proteins for control; B, elution buffer for MD-MMs; B1, the supernatant solution after the immobilization of crude proteins for MD-MMs. (c) Enrichment efficiency of MD-MMs at different binding time. (d) Binding capacity of MD-MMs after multiple rounds of recycling.

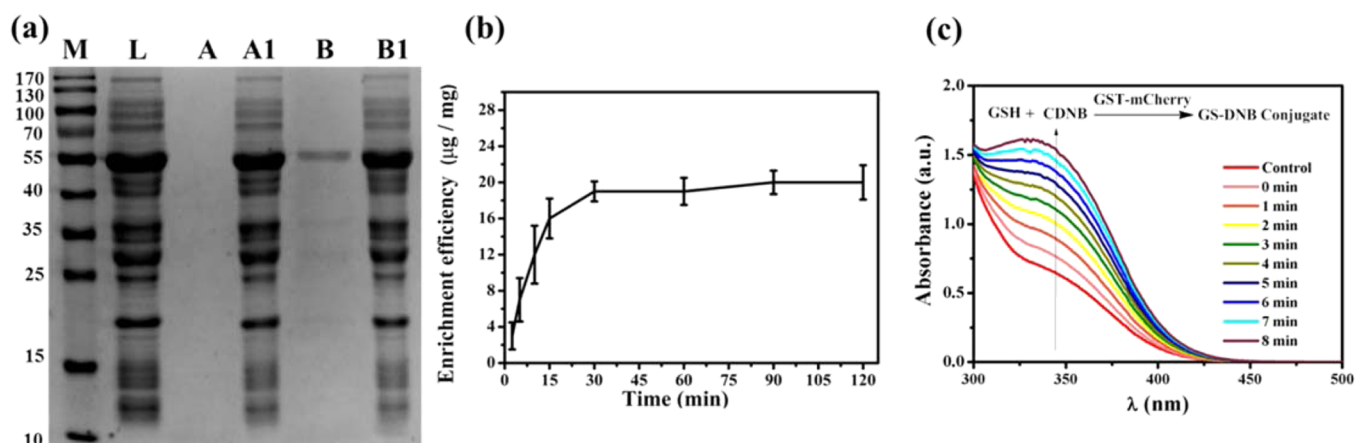


Figure 6. (a) SDS-PAGE analysis of GSH-MMs: lane M, marker; L, crude *E. coli* lysate; A, elution buffer for control; A1, the supernatant solution after the immobilization of crude proteins for control; B, elution buffer for GSH-MMs; B1, the supernatant solution after the immobilization of crude proteins for GSH-MMs. (b) Enrichment efficiency of GSH-MMs at different binding time. (c) Total activities of GST-mCherry detected by GST Assay Kit.

reacting its thiol with 3-bromo-1-propyne.⁴¹ Biotin was alkynylated by condensation reaction between its carboxyl group and 3-amino-1-propyne.⁴² BG was also alkynylated by acid–base condensation, by reacting its amine group with 5-hexynoic acid.⁴³ The alkynylated ligands then reacted with the azide groups on MMs by the click chemistry to obtain MD-, GSH-, biotin-, and BG-functionalized MMs. These four MMs with different affinity ligands on the surface were used for purification and immobilization of corresponding tagged proteins.^{44,45}

Separation and Purification of MBP-Fusion Protein. We first tested MD-MMs by purification of an MBP-tagged fluorescent protein (MBP-mCherry, with a molecular weight of ~70 kDa) directly from crude cell lysates (Figure 5a). The

cell lysates of MBP-mCherry proteins were incubated with MD-MMs. MD-MMs with the immobilized proteins were then separated from the lysates by magnetic separation and washed three times by MBP binding buffer. The proteins on the MD-MMs were eluted by maltose elution buffer and analyzed by SDS-PAGE (Figure 5b), along with the cell lysate and the eluted solutions collected at different stages. Figure 5b clearly shows that MBP-mCherry in cell lysates (Lane L) bound selectively on the MD-MMs and was extracted from the solution with high purity (Lane B). In contrast, no proteins were isolated if N₃-MMs were used in a control experiment (Lane A). Figure 5c shows that the adsorption can reach an equilibrium level within 15 min of incubation, with a binding capability of $25 \pm 2 \mu\text{g mg}^{-1}$ of MD-MMs. We examined the

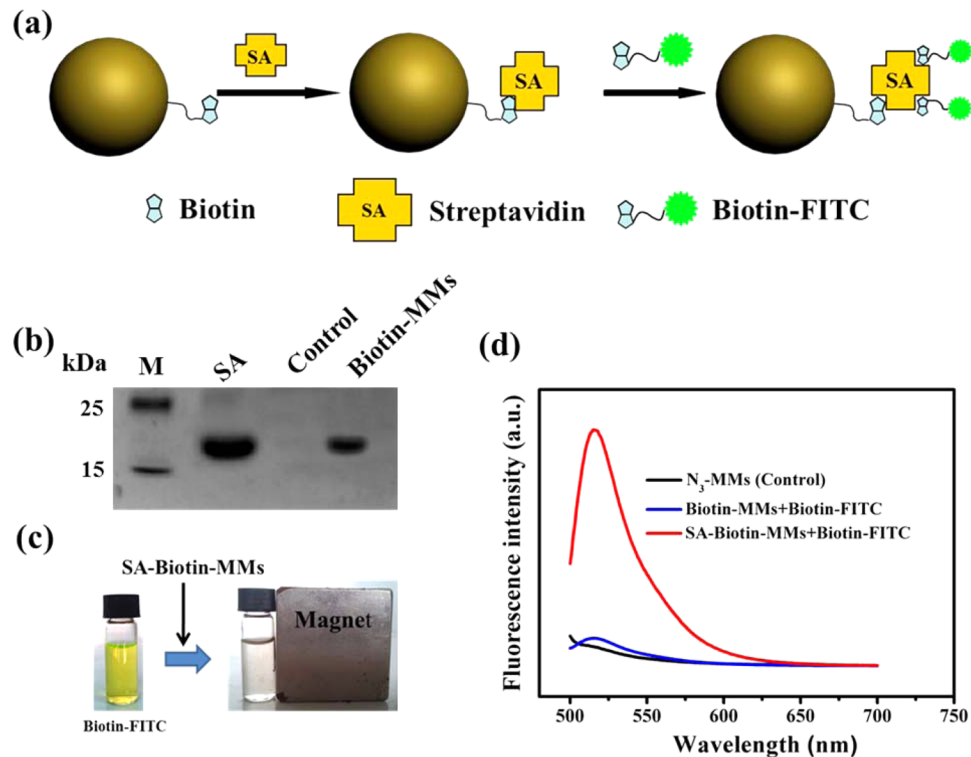


Figure 7. (a) Procedure of immobilization of SA on biotin-MMs and the detection of immobilized SA by biotin-FITC. (b) SDS-PAGE analysis of eluted SA from $\text{N}_3\text{-MMs}$ (control) and biotin-MMs. (c) Attachment of biotin-FITC on SA-biotin-MMs. (d) Fluorescence spectra of biotin-FITC bound SA-biotin-MMs (in red), and biotin-FITC incubated with biotin-MMs, which was fractionated before fluorescence measurement (in blue).

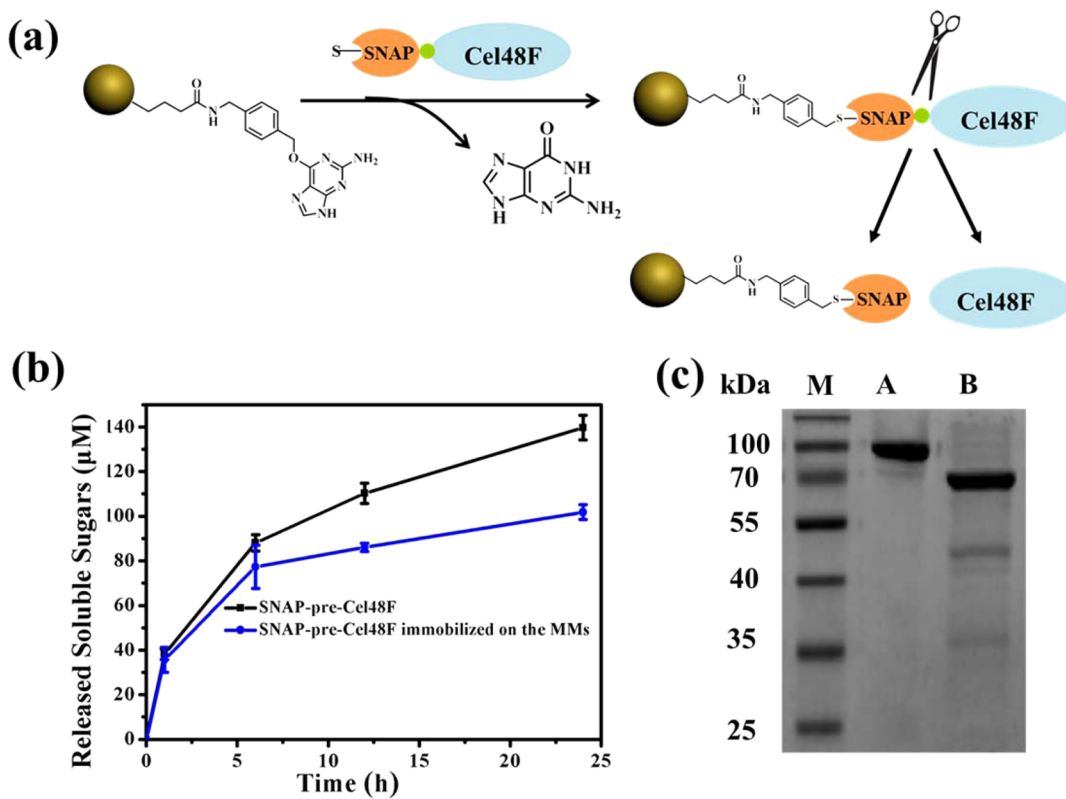


Figure 8. (a) Procedure of immobilization SNAP-pre-Cel48F on BG-MMs and the enzymatic cleavage of immobilized SNAP-pre-Cel48F to release Cel48F. (b) Avicel hydrolysis by SNAP-pre-Cel48F in free state or immobilized state. (c) SDS-PAGE analysis of purified SNAP-pre-Cel48F (lane A) and the Cel48F released from the cleavage of immobilized SNAP-pre-Cel48F by protease (lane B).

binding efficiency of MD-MMs with standard MBP-mCherry. The protein maximum adsorption of MD-MMs was $\sim 25 \mu\text{g mg}^{-1}$, and the binding efficiency was $\sim 70\%$. Figure 5d shows the change of binding capacities of the MD-MMs after repeated cycles of separation and elution of MBP-mCherry. The MD-MMs retain $>80\%$ of their binding capacity even after 5 cycles.

Separation and Purification of GST-Fusion Protein. To further demonstrate that the MMs platform is applicable to different ligand–protein interactions, we then examined the effectiveness of GSH-MMs for the purification of GST tagged mCherry (GST-mCherry). The purification and elution protocol was similar to that used for MD-MMs. Once again, by the specific ligand–protein interaction, GST-mCherry was readily purified from the cell lysates by the GSH-MMs (Figure 6a). Within 30 min of incubation, $20 \pm 2 \mu\text{g}$ of proteins were immobilized on 1 mg of GSH-MMs (Figure 6b). The protein maximum adsorption of GSH-MMs was $\sim 20 \mu\text{g mg}^{-1}$ for GST-mCherry, and the binding efficiency was nearly 60%. Furthermore, GST Assay Kit was chosen to measure the activity of the obtained GST-mCherry. As shown in Figure 6c, the conjugation of the thiol group of glutathione to the 1,3-dinitro-4-chlorobenzene was effectively catalyzed by the purified GST-mCherry as there was an obvious increase in the absorbance at 340 nm.³¹

Immobilization of Streptavidin. We then set up to test the MMs platform for multidomain proteins (streptavidin). Streptavidin (SA) has a four-domain structure, and the binding of biotin to SA is one of the strongest noncovalent interactions (Figure 7a).⁴⁶ The biotin-MMs worked very well to immobilize SA from the solution. Since the binding between biotin and SA is extremely tight, the immobilized SA on biotin-MMs needed to be boiled to elute SA for SDS-PAGE analysis (Figure 7b). The maximum adsorption of biotin-MMs was $\sim 25 \mu\text{g mg}^{-1}$ for SA, and the binding efficiency was nearly 90%. To find out whether the multidomain SA retains their folding and activity on the MMs, they were incubated with a biotin-modified fluorescein isothiocyanate (biotin-FITC). Figure 7c shows that 90% biotin-FITC attached to the unoccupied domains of SA that were immobilized on MMs and can be subsequently removed from the solution by magnetic separation. Prominent fluorescence was then found in the biotin-FITC bound SA-biotin-MMs (SA-biotin-MMs + biotin-FITC; see Figure 7d), but not in the control samples biotin-FITC incubated with biotin-MMs (biotin-MMs + biotin-FITC).

Immobilization of SNAP-Fusion Protein. Last, we tested the MMs for the covalent attachment of ligand with proteins (Figure 8a, between BG and SNAP tag⁴⁷). BG-MMs were used to immobilize a SNAP-tagged cellulolytic enzyme with a cleavable linker (SNAP-pre-Cel48F; see SNAP-pre-Cel48F CDS in Supporting Information for the amino acid sequence of the protein). We confirmed the immobilized efficiency of BG-MMs with standard SNAP-pre-Cel48F. The protein maximum adsorption of BG-MMs was $\sim 20 \mu\text{g mg}^{-1}$, and the binding efficiency was 90%. Once immobilized on BG-MMs, the activity of SNAP-pre-Cel48F was determined by evaluation of its enzymatic reaction on Avicel (20 mg mL^{-1}) using a ferricyanide assay.³² Figure 8b compares the amount of soluble sugars released at different time intervals by the same amount of proteins, either in the free state or in the attachment of BG-MMs. Clearly, the biological activity of Cel48F was largely retained on MMs. The PreScission protease was used to cleave the linker between SNAP tag and Cel48F after they were immobilized on BG-MMs. As was shown in the lane B of

Figure 8c, a clear band ($\sim 70 \text{ kDa}$) was found, which was assigned to the Cel48F part. The PreScission protease, which was a 47 kDa protein, could also be found in the lane B of Figure 8c. This further demonstrates the versatility of the ligand-functionalized MMs.

4. CONCLUSIONS

In summary, azide-functionalized MMs were developed as a generic, clickable platform for incorporation of a variety of capture ligands for purification and immobilization of recombinant proteins. The general applicability of the approach has been demonstrated by the incorporation of four alkynylated ligands on the surface of azide-MMs for fast and selective immobilization of corresponding proteins. The azide-functionalized MMs should be applicable for a variety of ligands and substrates that are amenable to alkynylation reactions.

■ ASSOCIATED CONTENT

5 Supporting Information

Preparation of O^6 -(4-aminomethyl-benzyl)guanine, the transformation method, and the amino acid sequences of MBP-mCherry, SNAP-pre-Cel48F, and GST-mCherry. This material is available free of charge via the Internet at <http://pubs.acs.org>.

■ AUTHOR INFORMATION

Corresponding Author

*Phone: +86-21-65642385. Fax: +86-21-65640293. E-mail: wlyang@fudan.edu.cn.

Author Contributions

The manuscript was written through contributions of all authors. All authors have given approval to the final version of the manuscript.

Notes

The authors declare no competing financial interest.

■ ACKNOWLEDGMENTS

We acknowledge the support from the National Natural Science Foundation of China (Grant Nos. 51473037 and 51273047) and the “Shu Guang” Project (12SG07) supported by Shanghai Municipal Education Commission and Shanghai Education Development Foundation.

■ REFERENCES

- (1) Laemmli, U. K. Cleavage of Structural Proteins during the Assembly of the Head of Bacteriophage T4. *Nature* **1970**, *227*, 680–685.
- (2) Yates, J. R.; Speicher, S.; Griffin, P. R.; Hunkapiller, T. Peptide Mass Maps: a Highly Informative Approach to Protein Identification. *Anal. Biochem.* **1993**, *214*, 397–408.
- (3) Carter, P. J. Introduction to Current and Future Protein Therapeutics: a Protein Engineering Perspective. *Exp. Cell Res.* **2011**, *317*, 1261–1269.
- (4) Waibel, R.; Alberto, R.; Willuda, J.; Finnern, R.; Schibli, R.; Stichelberger, A.; Egli, A.; Abram, U.; Mach, J. P.; Pluckthun, A.; Schubiger, P. A. Stable One-step Technetium-99m Labeling of His-tagged Recombinant Proteins with a Novel Tc(I)-carbonyl Complex. *Nat. Biotechnol.* **1999**, *17*, 897–901.
- (5) Singh, P. K.; Chan, P. F.; Hibbs, M. J.; Vazquez, M. J.; Segura, D. C.; Thomas, D. A.; Theobald, A. J.; Gallagher, K. T.; Hassan, N. J. High-yield Production and Characterization of Biologically Active GST-tagged Human Topoisomerase II α Protein in Insect Cells for the Development of a High-throughput Assay. *Protein Expression Purif.* **2011**, *76*, 165–172.

- (6) Maurel, D.; Comps-Agrar, L.; Brock, C.; Rives, M. L.; Bourrier, E.; Ayoub, M. A.; Bazin, H.; Tinel, N.; Durroux, T.; Prezeau, L.; Trinquet, E.; Pin, J. P. Cell-surface Protein-protein Interaction Analysis with Time-resolved FRET and Snap-tag Technologies: Application to GPCR Oligomerization. *Nat. Methods* **2008**, *5*, S61–S67.
- (7) Locatelli-Hoops, S.; Sheen, F. C.; Zoubak, L.; Gawrisch, K.; Yeliseev, A. A. Application of HaloTag Technology to Expression and Purification of Cannabinoid Receptor CB2. *Protein Expression Purif.* **2013**, *89*, 62–72.
- (8) Yang, Y.; Zhang, C. Y. Simultaneous Measurement of SUMOylation Using SNAP/CLIP-Tag-Mediated Translation at the Single-molecule Level. *Angew. Chem., Int. Ed.* **2013**, *52*, 691–694.
- (9) Walsh, G. Biopharmaceutical Benchmarks 2010. *Nat. Biotechnol.* **2010**, *28*, 917–924.
- (10) Guo, J.; Yang, W. L.; Wang, C. C. Magnetic Colloidal Supraparticles: Design, Fabrication and Biomedical Applications. *Adv. Mater.* **2013**, *25*, S196–S214.
- (11) Ma, W. F.; Zhang, Y.; Li, L. L.; You, L. J.; Zhang, P.; Zhang, Y. T.; Li, J. M.; Yu, M.; Guo, J.; Lu, H. J.; Wang, C. C. Tailor-Made Magnetic $\text{Fe}_3\text{O}_4@\text{mTiO}_2$ Microspheres with a Tunable Mesoporous Anatase Shell for Highly Selective and Effective Enrichment of Phosphopeptides. *ACS Nano* **2012**, *6*, 3179–3188.
- (12) Zhang, Y. T.; Li, L.; Ma, W.; Zhang, Y.; Yu, M.; Guo, J.; Lu, H.; Wang, C. C. Two-in-One Strategy for Effective Enrichment of Phosphopeptides Using Magnetic Mesoporous $\gamma\text{-Fe}_2\text{O}_3$ Nanocrystal Clusters. *ACS Appl. Mater. Interfaces* **2013**, *5*, 614–621.
- (13) Xu, S.; Song, X.; Guo, J.; Wang, C. C. Composite Microspheres for Separation of Plasmid DNA Decorated with MNPs through in Situ Growth or Interfacial Immobilization Followed by Silica Coating. *ACS Appl. Mater. Interfaces* **2012**, *4*, 4764–4775.
- (14) Zhang, Y. T.; Li, D.; Yu, M.; Ma, W. F.; Guo, J.; Wang, C. C. $\text{Fe}_3\text{O}_4/\text{PVIM-Ni}^{2+}$ Magnetic Composite Microspheres for Highly Specific Separation of Histidine-Rich Proteins. *ACS Appl. Mater. Interfaces* **2014**, *6*, 8836–8844.
- (15) Zhang, Y. T.; Yang, Y.; Ma, W. F.; Guo, J.; Lin, Y.; Wang, C. C. Uniform Magnetic Core/Shell Microspheres Functionalized with Ni^{2+} -Iminodiacetic Acid for One Step Purification and Immobilization of His-Tagged Enzymes. *ACS Appl. Mater. Interfaces* **2013**, *5*, 2626–2633.
- (16) Xu, F.; Geiger, J. H.; Baker, G. L.; Bruening, M. L. Polymer Brush-Modified Magnetic Nanoparticles for His-Tagged Protein Purification. *Langmuir* **2011**, *27*, 3106–3112.
- (17) Pan, Y.; Long, M. J. C.; Lin, H. C.; Hedstrom, L.; Xu, B. Magnetic Nanoparticles for Direct Protein Sorting Inside Live Cells. *Chem. Sci.* **2012**, *3*, 3495–3499.
- (18) You, C.; Chen, H.; Myung, S.; Sathitsuksanoh, N.; Ma, H.; Zhang, X. Z.; Li, J.; Zhang, Y. H. P. Enzymatic Transformation of Nonfood Biomass to Starch. *Proc. Natl. Acad. Sci. U.S.A.* **2013**, *110*, 7182–7187.
- (19) Kolb, H. C.; Finn, M. G.; Sharpless, K. B. Click Chemistry: Diverse Chemical Function from a Few Good Reactions. *Angew. Chem., Int. Ed.* **2001**, *40*, 2004–2021.
- (20) Ilyas, S.; Ilyas, M.; van der Hoorn, R. A. L.; Mathur, S. Selective Conjugation of Proteins by Mining Active Proteomes through Click-Functionalized Magnetic Nanoparticles. *ACS Nano* **2013**, *7*, 9655–9663.
- (21) Spurlino, J. C.; Lu, G. Y.; Quijano, F. A. The 2.3-A Resolution Structure of the Maltose- or Maltodextrin-Binding Protein, a Primary Receptor of Bacterial Active Transport and Chemotaxis. *J. Biol. Chem.* **1991**, *266*, 5202–5219.
- (22) Smith, D. B.; Johnson, K. S. Single-Step Purification of Polypeptides Expressed in Escherichia-Coli as Fusions with Glutathione S-Transferase. *Gene* **1988**, *67*, 31–40.
- (23) Weber, P. C.; Ohlendorf, D. H.; Wendoloski, J. J.; Salemme, F. R. Structural Origins of High-Affinity Biotin Binding to Streptavidin. *Science* **1989**, *243*, 85–88.
- (24) Klein, T.; Loeschberger, A.; Proppert, S.; Wolter, S.; van de Linde, S.; Sauer, M. Live-cell dSTORM with SNAP-tag Fusion Proteins. *Nat. Methods* **2011**, *8*, 7–9.
- (25) Ma, W. F.; Xu, S. A.; Li, J. M.; Guo, J.; Lin, Y.; Wang, C. C. Hydrophilic Dual-Responsive Magnetite/PMAA Core/Shell Microspheres with High Magnetic Susceptibility and pH Sensitivity via Distillation-Precipitation Polymerization. *J. Polym. Sci., Part A: Polym. Chem.* **2011**, *49*, 2725–2733.
- (26) Zheng, J.; Ma, C.; Sun, Y.; Pan, M.; Li, L.; Hu, X.; Yang, W. L. Maltodextrin-Modified Magnetic Microspheres for Selective Enrichment of Maltose Binding Proteins. *ACS Appl. Mater. Interfaces* **2014**, *6*, 3568–3574.
- (27) Pan, M.; Sun, Y.; Zheng, J.; Yang, W. L. Boronic Acid-Functionalized Core-Shell-Shell Magnetic Composite Microspheres for the Selective Enrichment of Glycoprotein. *ACS Appl. Mater. Interfaces* **2013**, *5*, 8351–8358.
- (28) Susumu, K.; Mei, B. C.; Matoussi, H. Multifunctional Ligands Based on Dihydrolipoic Acid and Polyethylene Glycol to Promote Biocompatibility of Quantum Dots. *Nat. Protoc.* **2008**, *4*, 424–436.
- (29) ReverbelLeroy, C.; Pages, S.; Belaich, A.; Belaich, J. P.; Tardif, C. The Processive Endocellulase CelF, a Major Component of the Clostridium Cellulolyticum Cellulosome: Purification and Characterization of the Recombinant Form. *J. Bacteriol.* **1997**, *179*, 46–52.
- (30) Compton, S. J.; Jones, C. G. Mechanism of Dye Response and Interference in the Bradford Protein Assay. *Anal. Biochem.* **1985**, *236*, 369–374.
- (31) Habig, W. H.; Pabst, M. J.; Jakoby, W. B. Glutathione S-Transferases - First Enzymatic Step in Mercapturic Acid Formation. *J. Biol. Chem.* **1974**, *249*, 7130–7139.
- (32) Park, J. T.; Johnson, M. J. A Submicrodetermination of Glucose. *J. Biol. Chem.* **1949**, *181*, 149–151.
- (33) Xuan, S. H.; Wang, Y. X. J.; Yu, J. C.; Leung, K. C. F. Tuning the Grain Size and Particle Size of Superparamagnetic Fe_3O_4 Microparticles. *Chem. Mater.* **2009**, *21*, 5079–5087.
- (34) Na, B. H.; Palui, G.; Rosenberg, J. T.; Jin, X.; Grant, S. C.; Matoussi, H. Multidentate Catechol-Based Polyethylene Glycol Oligomers Provide Enhanced Stability and Biocompatibility to Iron Oxide Nanoparticles. *ACS Nano* **2012**, *6*, 389–399.
- (35) Droumaguet, B. L.; Nicolas, J.; Brambilla, D.; Mura, S.; Maksimenko, A.; Kimpe, L. D.; Salvati, E.; Zona, C.; Airoldi, C.; Canovi, M.; Gobbi, M.; Noiray, M.; Ferla, B. L.; Nicotra, F.; Scheper, W.; Flores, O.; Masserini, M.; Andrieux, K.; Couvreur, P. Versatile and Efficient Targeting Using a Single Nanoparticulate Platform: Application to Cancer and Alzheimer's Disease. *ACS Nano* **2012**, *7*, 5866–5879.
- (36) Pan, Y.; Chen, Y.; Wang, D.; Wei, C.; Guo, J.; Lu, D.; Chu, C.; Wang, C. C. Redox/pH dual stimuli-responsive biodegradable nanohydrogels with varying responses to dithiothreitol and glutathione for controlled drug release. *Biomaterials* **2012**, *33*, 6570–6579.
- (37) Chu, B.; Wang, Z. L.; Yu, J. Q. Dynamic Light Scattering Study of Internal Motions of Polymer Coils in Dilute Solution. *Macromolecules* **1991**, *24*, 6832–6838.
- (38) Deng, H.; Li, X. L.; Peng, Q.; Wang, X.; Chen, J. P.; Li, Y. D. Monodisperse Magnetic Single-Crystal Ferrite Microspheres. *Angew. Chem., Int. Ed.* **2005**, *44*, 2782–2785.
- (39) Besanceney-Webler, C.; Jiang, H.; Zheng, T.; Feng, L.; Soriano del Amo, D.; Wang, W.; Klivansky, L.; Marlow, F.; Liu, Y.; Wu, P. Increasing the Efficacy of Bioorthogonal Click Reactions for Bioconjugation: A Comparative Study. *Angew. Chem., Int. Ed.* **2011**, *50*, 8051–8056.
- (40) van Wijk, A.; Siebum, A.; Schoevaart, R.; Kieboom, T. Enzymatically Oxidized Lactose and Derivatives Thereof as Potential Protein Cross-Linkers. *Carbohydr. Res.* **2006**, *341*, 2921–2926.
- (41) Vala, C.; Chrétien, F.; Balentova, E.; Lamandé-Langle, S.; Chapleur, Y. Neoglycopeptides through Direct Functionalization of Cysteine. *Tetrahedron Lett.* **2011**, *52*, 17–20.
- (42) Borcard, F.; Godinat, A.; Staedler, D.; Blanco, H. C.; Dumont, A.; Chapuis-Bernasconi, C.; Scaletta, C.; Applegate, L. A.; Juillerat, F. K.; Gonzenbach, U.; Gerber-Lemaire, S.; Juillerat-Jeanneret, L. Covalent Cell Surface Functionalization of Human Fetal Osteoblasts for Tissue Engineering. *Bioconjugate Chem.* **2011**, *22*, 1422–1432.

- (43) Mei, D.; Qu, Y.; He, J.; Chen, L.; Yao, Z. Syntheses and Characterizations of Novel Pyrrolocoumarin Probes for SNAP-tag Labeling Technology. *Tetrahedron* **2011**, *67*, 2251–2259.
- (44) Riente, P.; Yadav, J.; Pericas, M. A. A Click Strategy for the Immobilization of MacMillan Organocatalysts onto Polymers and Magnetic Nanoparticles. *Org. Lett.* **2012**, *14*, 3668–3671.
- (45) Cui, Q.; Hou, Y.; Hou, J.; Pan, P.; Li, L.; Bai, G.; Lou, G. Preparation of Functionalized Alkynyl Magnetic Microspheres for the Selective Enrichment of Cell Glycoproteins Based on Click Chemistry. *Biomacromolecules* **2013**, *14*, 124–131.
- (46) Green, N. M. Avidin. *Adv. Protein Chem.* **1975**, *29*, 85–133.
- (47) Mie, M.; Naoki, T.; Uchida, K.; Kobatake, E. Development of a Split SNAP-tag Protein Complementation Assay for Visualization of Protein-Protein Interactions in Living Cells. *Analyst* **2012**, *137*, 4760–4765.